Figure S1 SA-β-gal staining in replicative senescence and oncogene-induced senescence. **a,** MRC-5 and WI-38 fibroblasts at early passage (upper panels) and at replicative senescence (lower panels). **b**, MRC-5 and WI-38 retrovirally transduced with vector control (upper panels) and pBabe-Puro *ras* (H-*Ras*V12)[1] (lower panels). Note that premature senescence by POT1 knockdown was induced and confirmed by SA-β-gal staining as described in our previous study[2]. The dominant-negative TRF2-induced senescence was also as previously described by us[3] and others[4].

Figure S2 Regulation of miR-34a expression by p53 and its isoforms. **a,** hTERT-immortalized human fibroblasts (hTERT/NHF)[5] transduced with the shRNA knockdown vector targeting p53[6] (left) or treated with 10 μM of Nutlin-3a for 36 h[7] (right) were examined for miR-34a expression, as in Fig. 2a. The data (mean ± s.d. from triplicate sample) are shown as the relative expression levels to control cells (-). **b,** Luciferase reporter assay of the miR-34a promoter activity. p53-null MDAH041 cells were retrovirally transduced with p53 isoforms [control vector (-), p53β (β) or Δ133p53 (Δ133)] and transfected with full-length p53-expressing plasmids [control vector (-), wild-type (wt) or 273H mutant (mut)], miR-34a promoter-luciferase constructs [wild-type (upper panel) or mutated at the p53-binding site (lower panel)], as indicated, and pRL-SV40 (control plasmid driving *Renilla* luciferase). Promoter activities were measured as firefly luciferase activities normalized with *Renilla* luciferase activities. Data are mean ± s.d. from quaduplicate samples. ∗, $p < 0.01$. ∗∗, $p < 0.00001$. **c,** miR-34a is not upregulated at Δ133p53 knockdown- or p53β overexpression-induced senescence. MRC-5 (upper panel) and WI-38 (lower panel) at early passage (Y) were transfected with siRNA (control, Δ133si-1 or Δ133si-2, as in Fig. 3 and Supplementary Fig. S3) or transduced with retroviral overexpression constructs (vector control or p53β, as in Fig. 4a-c) and examined for miR-34a expression by qRT-PCR, as in Fig. 2a. Replicatively senescent cells (R.S., -, -) were included as the positive control. The data (mean ± s.d. from triplicate sample) are shown as the relative expression levels to untreated early-passage cells (Y, -, -).

Figure S3 Knockdown of endogenous Δ133p53 induces cellular senescence. Early-passage MRC-5 fibroblasts (at passage 32) were transfected with the siRNAs targeting Δ133p53 (Δ133si-1 and Δ133si-2) and a control oligonucleotide and examined in immunoblot analyses (**a**), SA-β-gal assay (**b**) and BrdU incorporation assay (**c**), as performed in Fig. 3. ∗, $p < 0.001$. **d,** No induction of apoptosis by Δ133p53 knockdown. MRC-5 and WI-38 transfected with control, Δ133si-1 and Δ133si-2 oligonucleotides were examined for caspase-3 (top) and PARP (middle, short and long exposure) in immunoblot. RKO cells treated with doxorubicin (DOX) were included as the positive control showing apoptosis. β-actin was a loading control (bottom). No cleaved caspase-3 or PARP was observed in Δ133p53-knocked-down fibroblasts.

Figure S4 Real-time qRT-PCR analysis of p53 target genes in p53β overexpression-induced cellular senescence. The expression levels in the p53β-overexpressing cells (FLAG-p53β) are shown as the relative values to those in control cells (Vector). Data are mean ± s.d. from triplicate samples. ∗, $p < 0.05$. ∗∗, $p < 0.01$.

Figure S5 p53β overexpression induces cellular senescence in human fibroblasts with ectopically expressed telomerase. **a**, Effects of p53β on cell proliferation. hTERT/NHF cells[5] were transduced with the retroviral vector driving FLAG-tagged p53β or control vector (a zeocin-resistant version). Cell proliferation assay was carried out as in Fig. 4b. **b**, Upregulation of $p21^{WAF1}$ by p53β overexpression. **c**, Representative pictures of SA-β-gal staining. **d**, Summary of SA-β-gal staining. The data were mean ± s.d. from three independent experiments. ∗, $p < 0.01$.

Figure S6 Δ133p53 overexpression extends the replicative lifespan in human fibroblasts. Late-passage MRC-5 (at passage 55) and WI-38 (at passage 53) were transduced with the FLAG-Δ133p53 retroviral vector or the control vector and examined for the cumulative PDL, as in Fig. 4d.

Figure S7 Immunoblot analyses of $p16^{INK4a}$, Δ133p53 and p53β in human colon adenomas. Eight cases of matched non-adenoma (N) and adenoma (A) tissues were examined for $p16^{INK4A}$, Δ133p53 (**a**) and p53β (**b**). β-actin was the control for normalization. Sixteen and 10 percent SDS-PAGE gels were used in (**a**) and (**b**), respectively. Bi-directional arrows indicate the positions of p53β bands. The data shown in Fig. 5b and 5c (Non-ad and Ad), as well as in **c** below, were from the quantitative analysis of these results. **c,** Paired t-test analyses of $p16^{INK4a}$, Δ133p53 and p53β expression in matched colon adenoma and non-adenoma tissues. The vertical axes are the expression levels normalized with β-actin. The p-values are in the parentheses. Case 1, aqua; case 2, blue; case 3, cyan; case 4, yellow; case 5, lavender; case 6, navy; case 7, purple; and case 8, brown.

Figure S8 Immunoblot analyses of Δ133p53 and p53β in human colon carcinomas. Twenty-nine cases of matched colon carcinoma (T) and non-carcinoma (N) tissues (Supplementary Table S3) were examined in immunoblot for Δ133p53 expression using 16% SDS-PAGE gels (**a**) and p53β expression using 10% SDS-PAGE gels (**b**). β-actin was the control for normalization. Arrows indicate the positions of p53β bands. Normal colon, non-adenoma and/or adenoma samples were included in each blot for quantitative comparison among different blots and different histopathological types. The data shown in Fig. 5c (Non-ca and Ca), 5d (Carcinoma, stage I, II and III) and 5e, as well as in **c** and **d** below, were from the quantitative analysis of these results. **c and d,** Paired t-test analyses of Δ133p53 and p53β expression in p53 'wild-type' *versus* 'mutant' cases of colon carcinomas. Twenty-eight cases of colon carcinomas were classified into two subgroups assumedly with 'wild-type' (n = 16) and 'mutant' p53 (n = 12), based on the immunohistochemical staining of p53 and MDM2[8, 9] (Supplementary Table S3). In each subgroup, the expression levels of Δ133p53 (**c**) and p53β (**d**) were compared between non-carcinoma (Non-ca) and carcinoma tissues by paired t-test. The vertical axes are the expression levels normalized with β-actin. The p-values are in the parentheses. The p53 'wild-type' carcinomas, but not "mutant" carcinomas, expressed significantly higher levels of Δ133p53. p53β was significantly less abundant in carcinoma tissues in both

subgroups because of the marked increase in non-carcinoma tissues (Fig. 5c). The actual values in each of the 28 cases are shown in Supplementary Table S4.

Figure S9 p53β and Δ133p53 are subject to different mechanisms of protein turnover and differentially regulated by full-length p53. **a**, mRNA expression of full-length p53, p53β and Δ133p53 in early-passage (Y) and senescent (S) fibroblasts. The same sets of cells as in Fig. 1b were analyzed by RT-PCR. For Δ133p53, the lower bands corresponded to the reported Δ133p53 sequences (GenBank DQ186650) and the upper bands were from mRNA with intron 5 unspliced. GAPDH was an internal control. **b**, Proteasomal degradation of full-length p53 and p53β, but not Δ133p53. The same sets of cells as in Fig. 1b were treated with 15 μM of the proteasomal inhibitor MG-132 for 8 h (+) and examined for full-length p53, Δ133p53 and p53β expression. -, untreated cells. β-actin was a loading control. **c**, Differential regulation of p53β and Δ133p53 by full-length p53. Early-passage fibroblasts were retrovirally transduced with the full-length (FL) p53 overexpression construct (+) and examined for p53β and Δ133p53 expression. -, cells transduced with control vector. β-actin was a loading control.

Figure S10 Full scan of immunoblots. **a,** Figure 1b. The rectangular areas of the blots were put together and shown in Fig. 1b as the results of TLQ40, MAP4, CM1 and DO-12 antibodies. The lanes between Y (early passage) and S (senescent) contained protein samples from intermediate passage numbers (MRC-5 at passage 43 and WI-38 at passage 46). **b,** Figure 3a.

Supplementary References

1. Serrano, M., Lin, A. W., McCurrach, M. E., Beach, D. & Lowe, S. W. Oncogenic ras provokes premature cell senescence associated with accumulation of p53 and p16INK4a. *Cell* **88**, 593-602 (1997).
2. Yang, Q. *et al*. Functional diversity of human protection of telomeres 1 isoforms in telomere protection and cellular senescence. *Cancer Res.* **67**, 11677-11686 (2007).
3. Yang, Q., Zheng, Y. L. & Harris, C. C. POT1 and TRF2 cooperate to maintain telomeric integrity. *Mol. Cell. Biol.* **25**, 1070-1080 (2005).
4. van Steensel, B., Smogorzewska, A. & de Lange, T. TRF2 protects human telomeres from end-to-end fusions. *Cell* **92**, 401-413 (1998).
5. Sengupta, S. *et al*. BLM helicase-dependent transport of p53 to sites of stalled DNA replication forks modulates homologous recombination. *EMBO J.* **22**, 1210-1222 (2003).
6. Brummelkamp, T. R., Bernards, R. & Agami, R. A system for stable expression of short interfering RNAs in mammalian cells. *Science* **296**, 550-553 (2002).
7. Kumamoto, K. *et al*. Nutlin-3a activates p53 to both down-regulate inhibitor of growth 2 and up-regulate mir-34a, mir-34b, and mir-34c expression, and induce senescence. *Cancer Res.* **68**, 3193-3203 (2008).
8. Costa, A. *et al.* p53 gene point mutations in relation to p53 nuclear protein accumulation in colorectal cancers. *J. Pathol.* **176**, 45-53 (1995).
9. Nenutil, R. *et al*. Discriminating functional and non-functional p53 in human tumours by p53 and MDM2 immunohistochemistry. *J. Pathol.* **207**, 251-259 (2005).

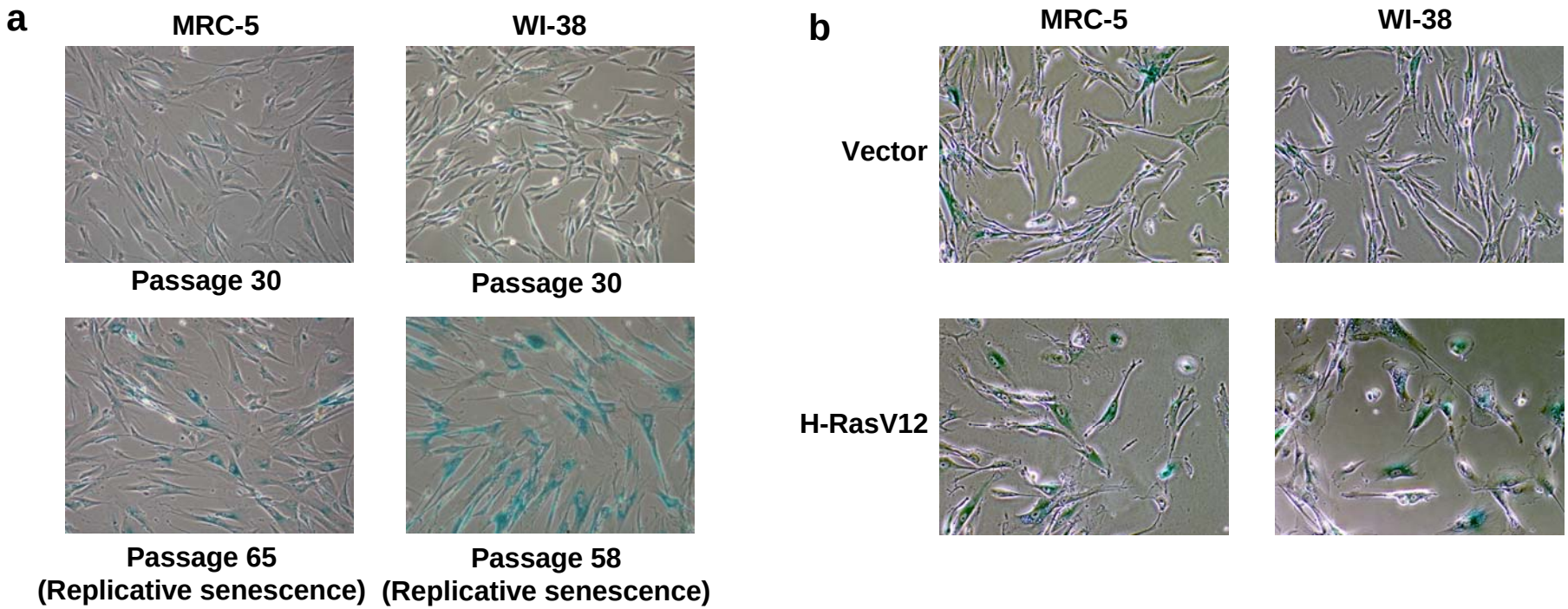

Supplementary Figure S1. SA-β-gal staining in replicative senescence and oncogene-induced senescence.

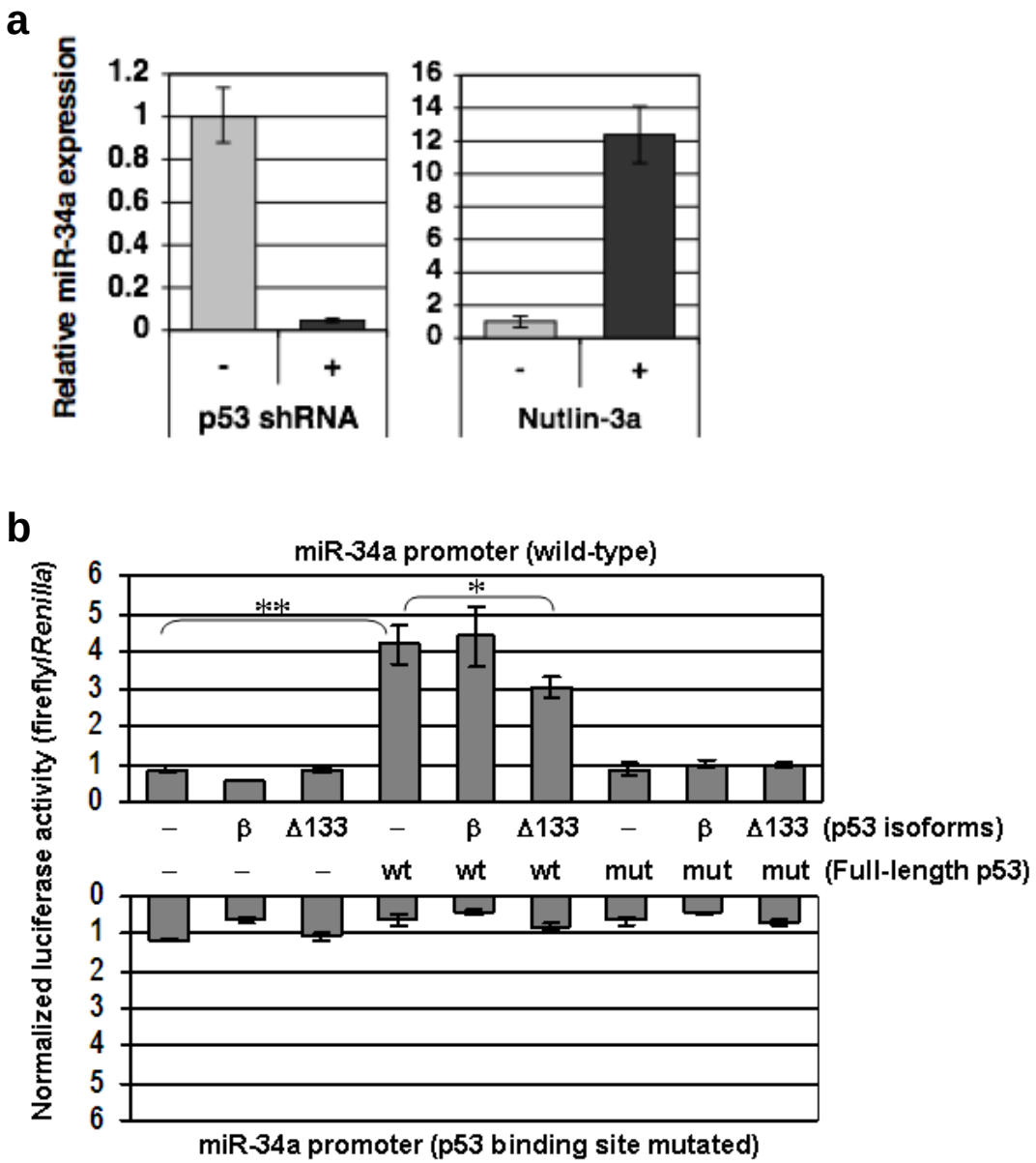

Supplementary Figure S2. Regulation of miR-34a expression by p53 and its isoforms.

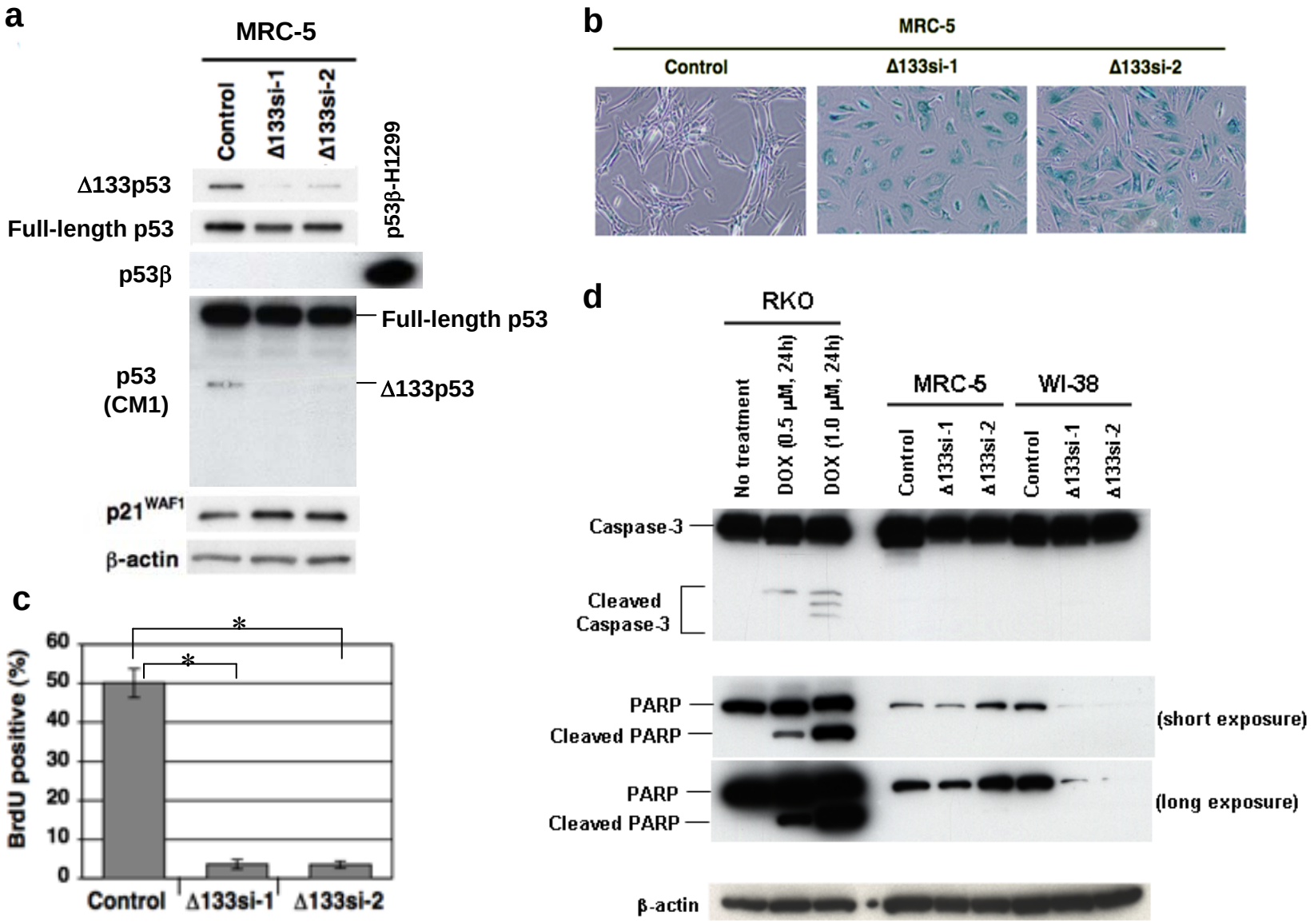

Supplementary Figure S3. Knockdown of endogenous Δ133p53 induces cellular senescence.

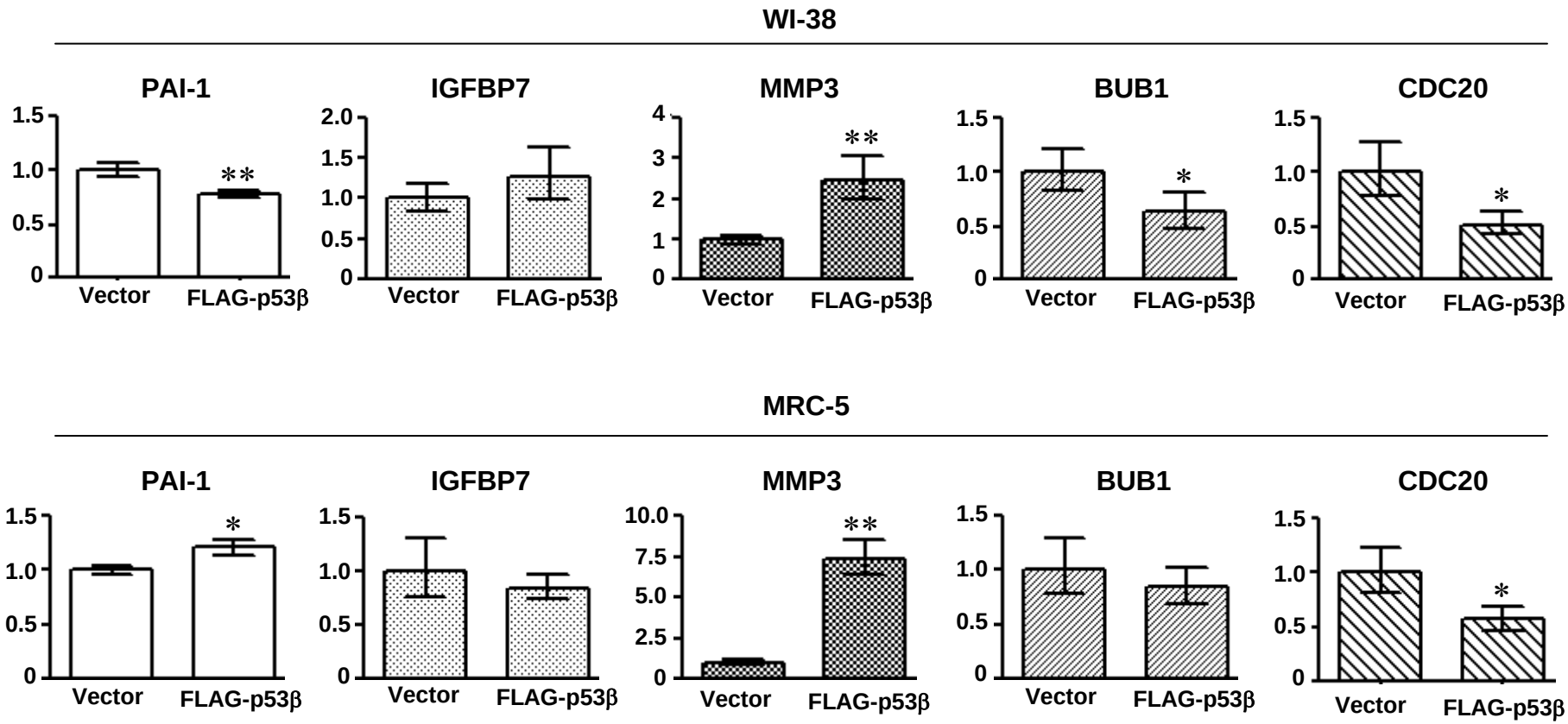

Supplementary Figure S4. qRT-PCR analysis of p53 target genes in p53β overexpression-induced cellular senescence.

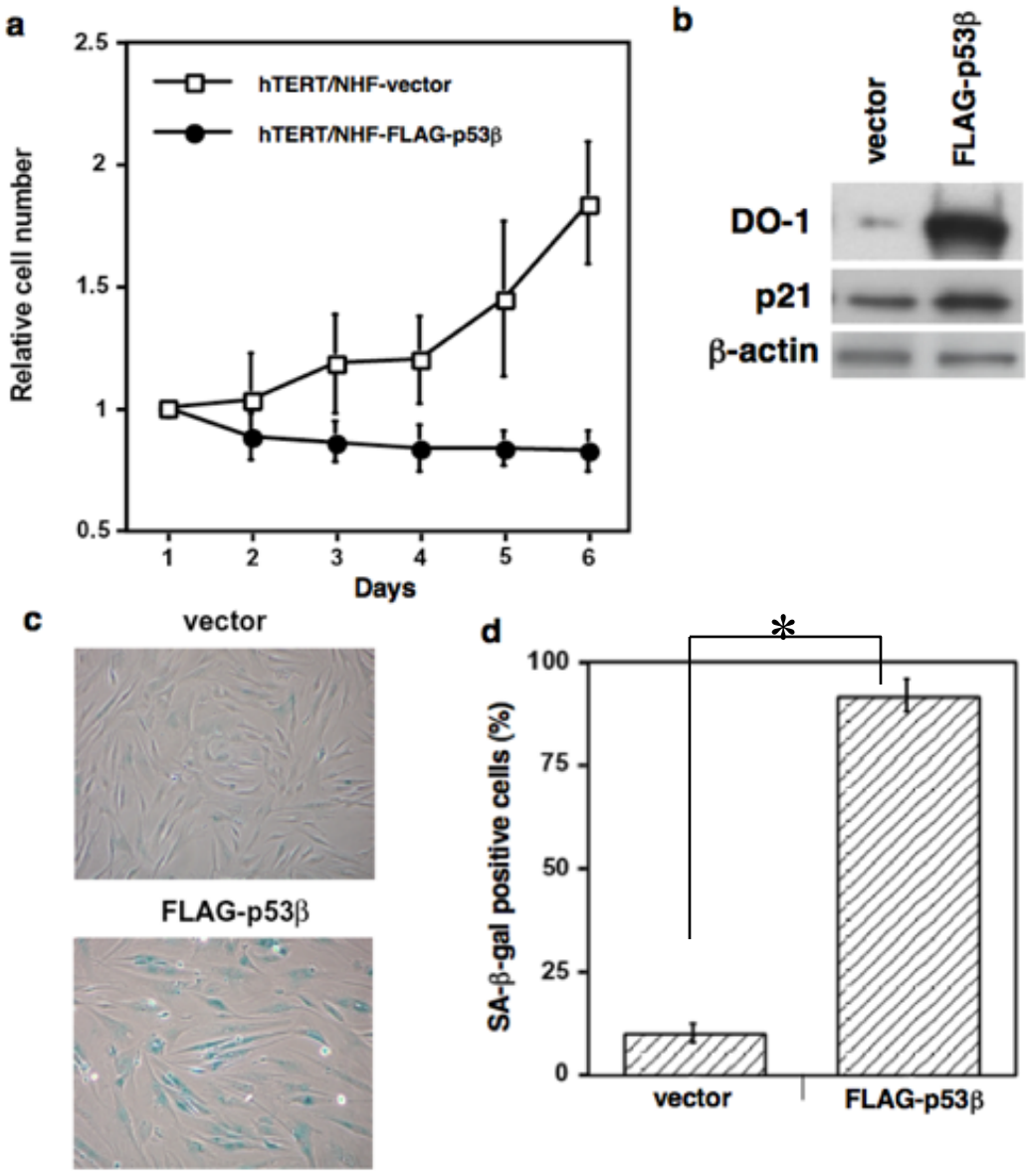

Supplementary Figure S5. p53β overexpression induces cellular senescence in human fibroblasts with ectopically expressed telomerase.

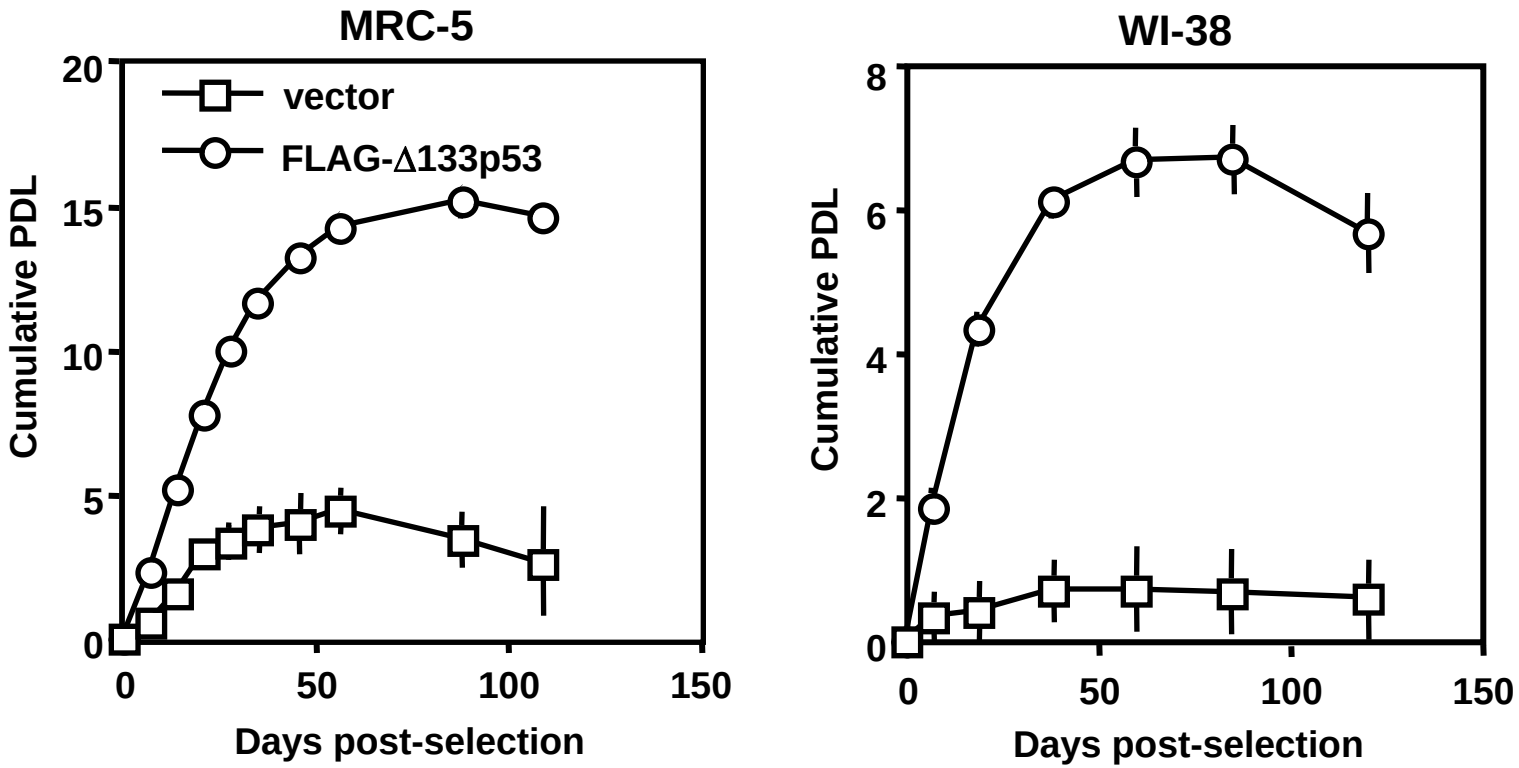

Supplementary Figure S6. Δ133p53 overexpression extends the replicative lifespan in human fibroblasts.

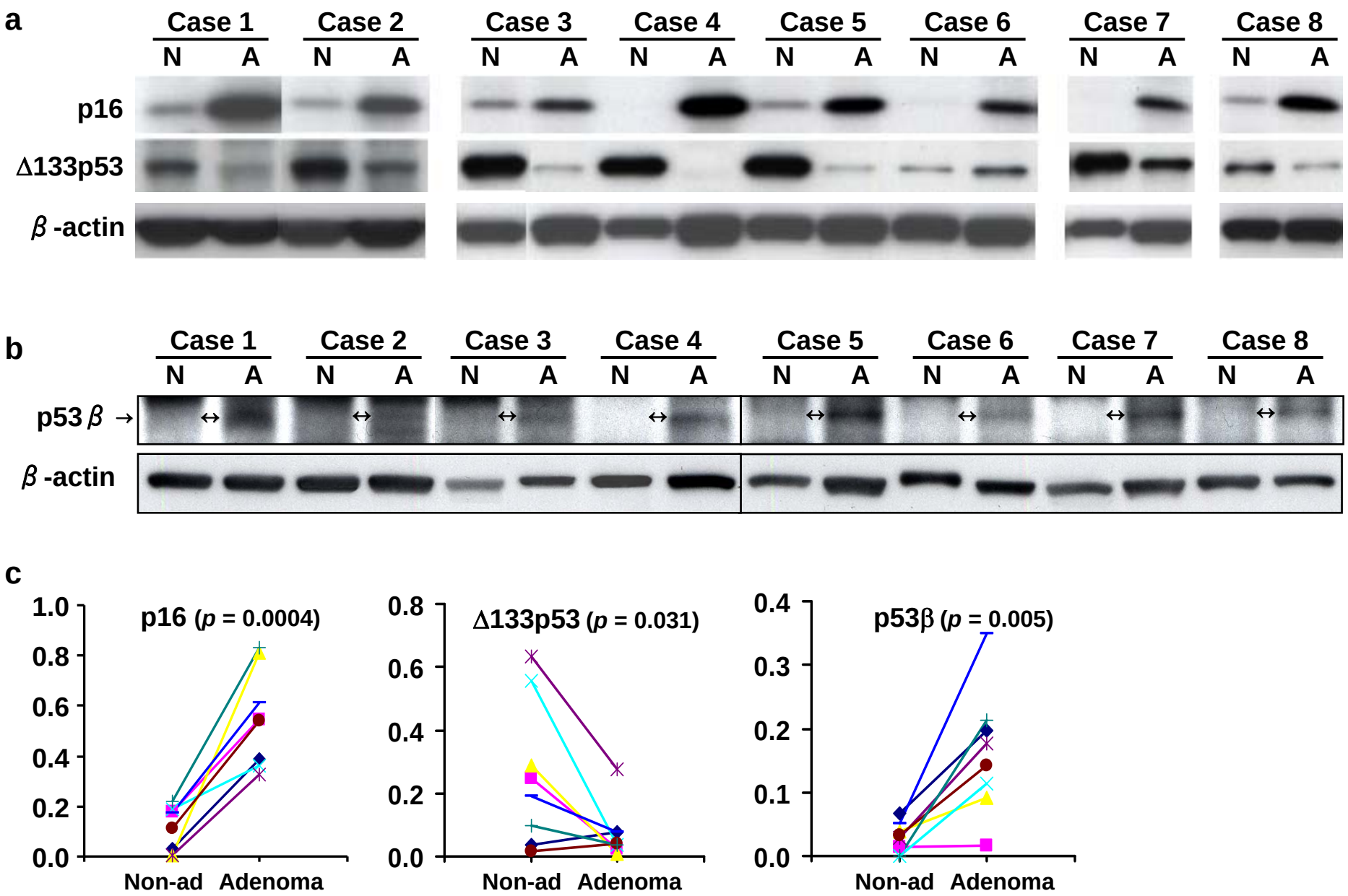

Supplementary Figure S7. Immunoblot analyses of p16^{INK4a}, Δ133p53 and p53β in human colon adenomas.

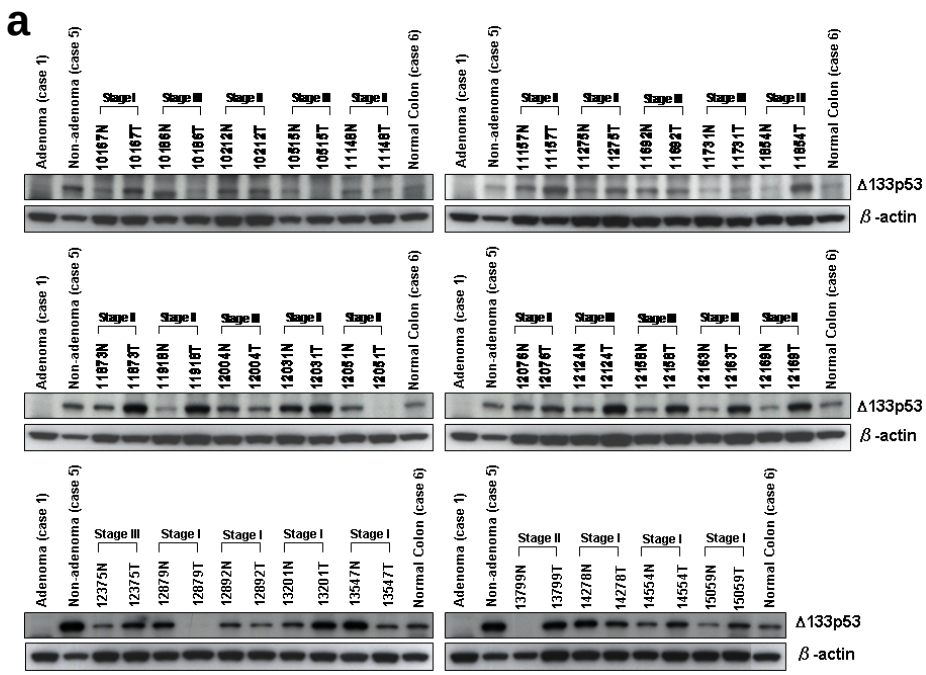

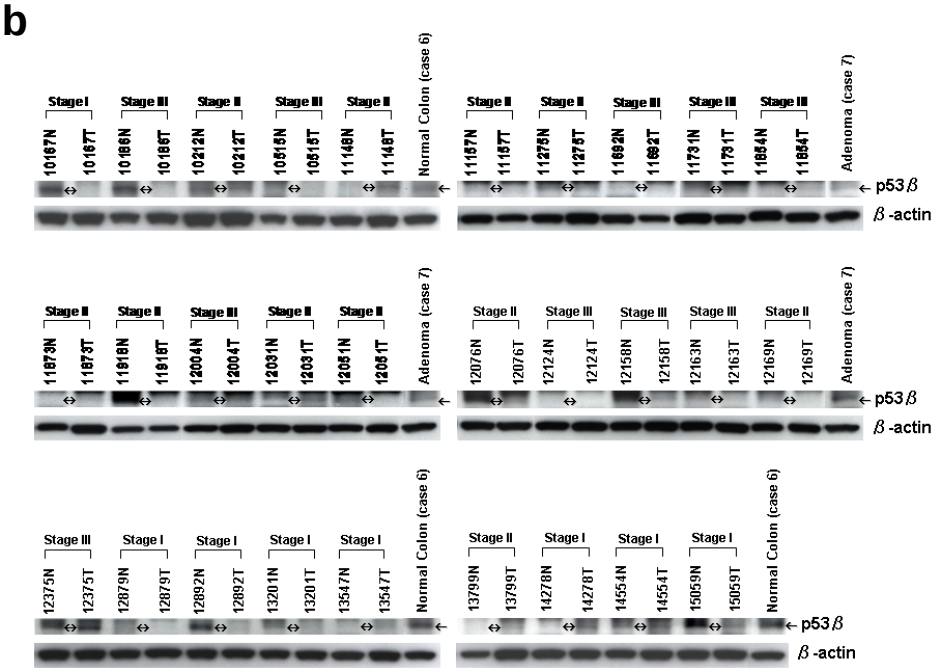

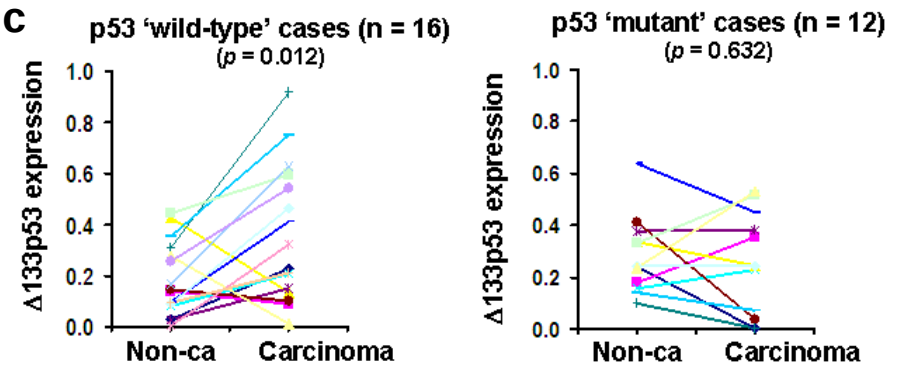

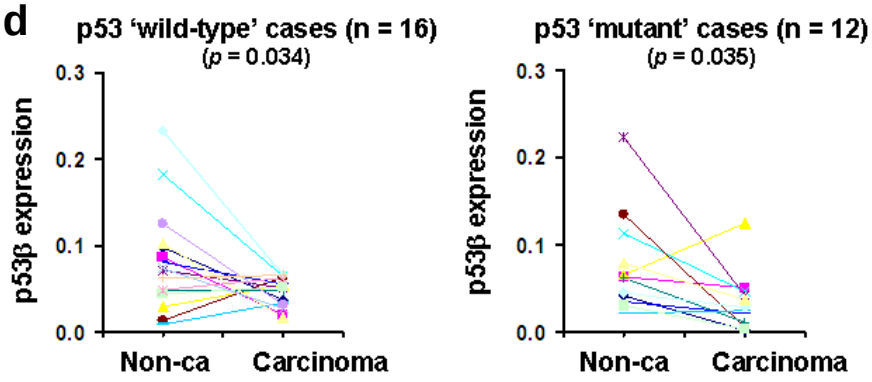

Supplementary Figure S8. Immunoblot analyses of Δ133p53 and p53β in human colon carcinomas.

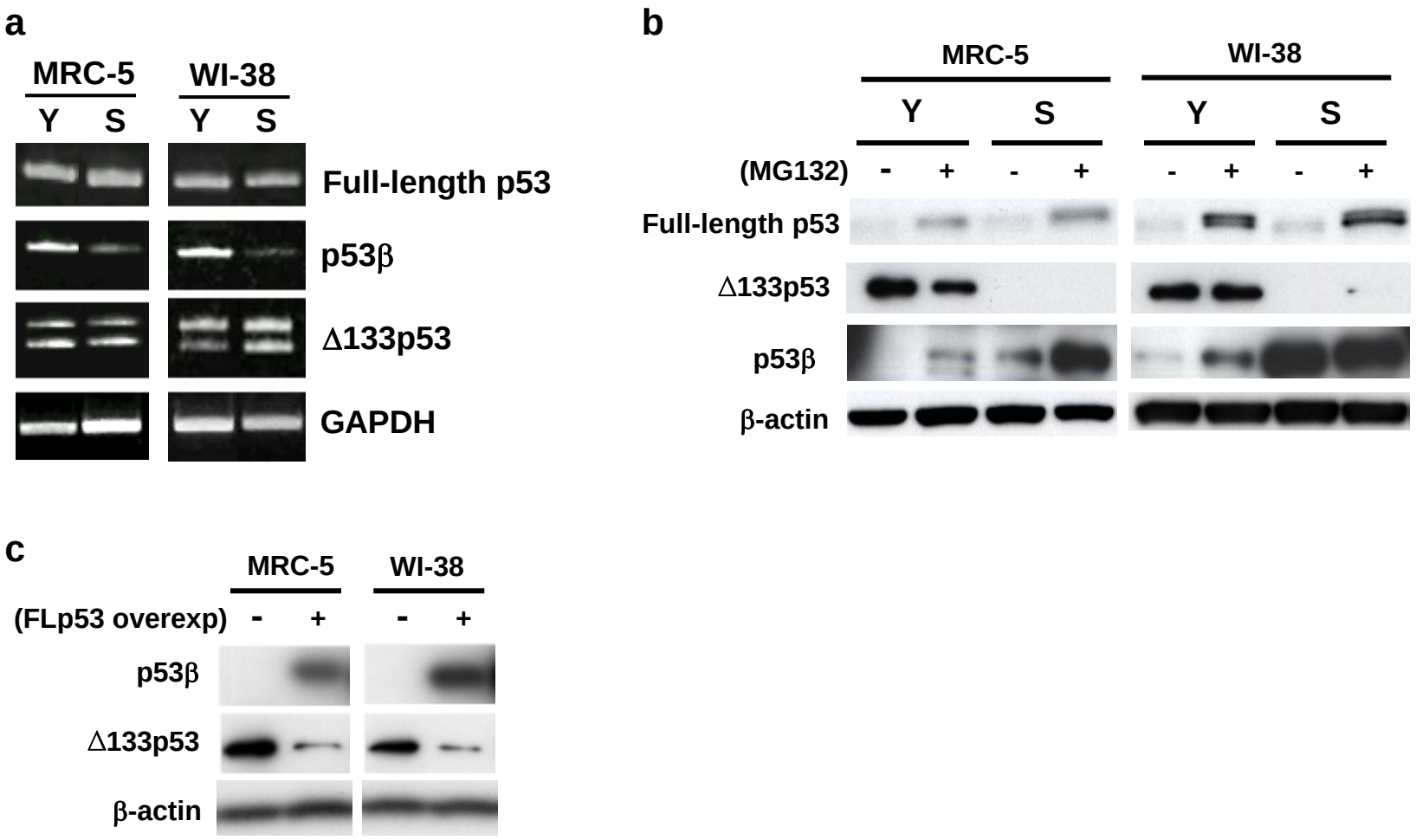

Supplementary Figure S9. p53β and Δ133p53 are subject to different mechanisms of protein turnover and differentially regulated by full-length p53.

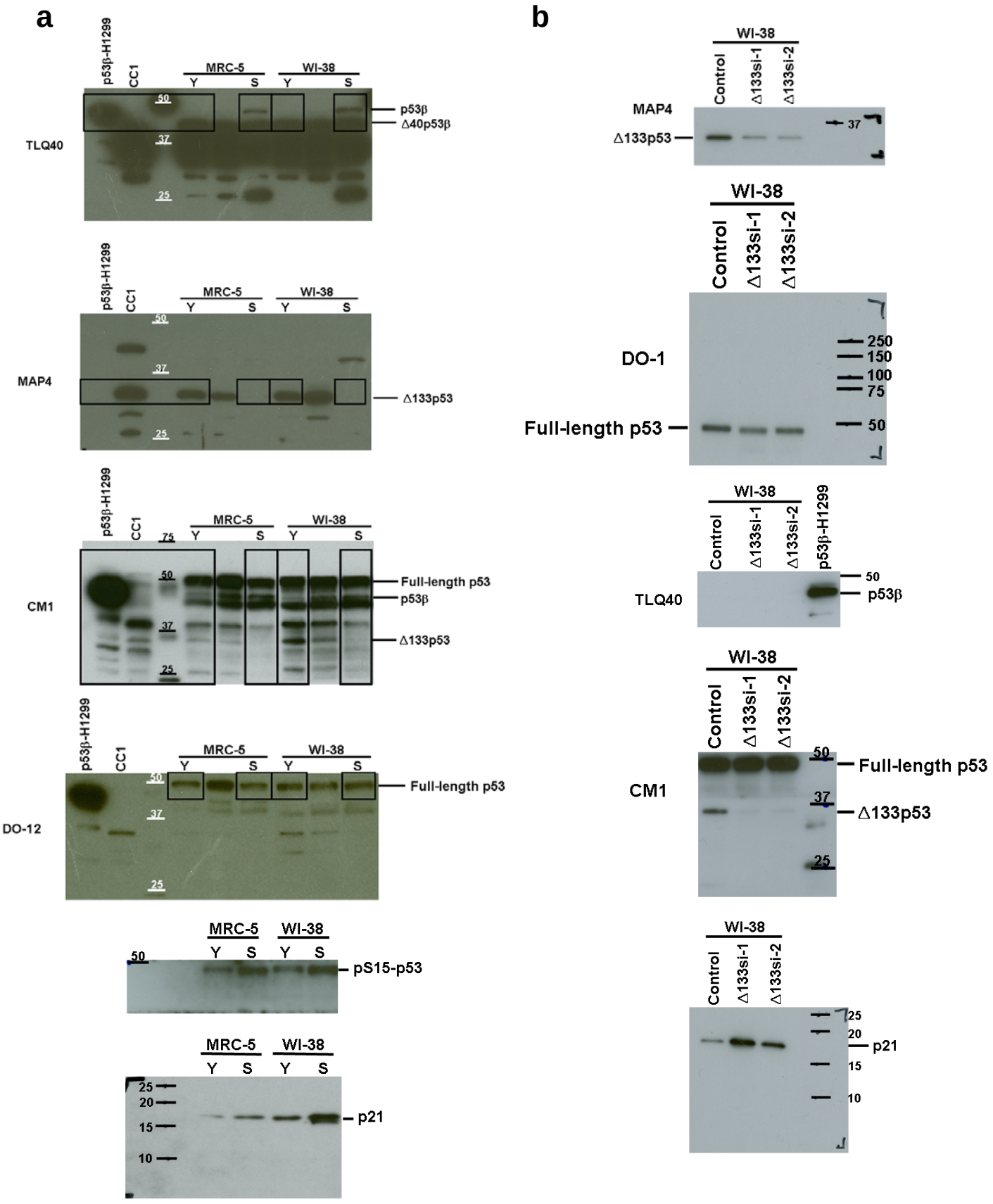
a
p53β-H1299
CC1
MRC-5
WI-38
Y
S
TLQ40
p53β
Δ40p53β
MAP4
Δ133p53
CM1
Full-length p53
DO-12
pS15-p53
p21
b
Control
Δ133si-1
Δ133si-2
DO-1
TLQ40
CM1
50
37
25
250
150
100
75
20
15
10

Supplementary Table S1.
Information on normal colon samples obtained from immediate autopsy.

Case number	Age	Gender	Cause of death
1	25	Male	Gun shot wound
2	29	Male	Gun shot wound
3	16	Female	Motor vehicle accident (closed head injury)
4	28	Male	Closed head injury
5	23	Female	Motor vehicle accident (closed head injury)
6	52	Female	Motor vehicle accident
7	76	Female	Motor vehicle accident
8	20	Male	Motor vehicle accident
9	19	Female	Gun shot wound

Supplementary Table S2.
Information on 8 pairs of colon adenoma and non-adenoma samples.

Case number	Age	Gender	Histopathological diagnosis
1	62	Male	Tubular adenoma
2	64	Female	Tubular adenoma
3	87	Female	Villous adenoma
4	84	Male	Villous adenoma
5	78	Male	Tubulovillous adenoma
6	66	Male	Tubular adenoma
7	79	Male	Villous adenoma
8	78	Male	Tubulovillous adenoma

Supplementary Table S3. Information on 29 cases of colon carcinoma.

Case*	Gender	Age	Stage	p53 status**	Histology	Survival (months)
10167	M	55	I	wild-type	adeno	154.0
10186	F	70	III	mutant	adeno	153.6
10212	F	66	II	wild-type	mucinous	144.3
10515	M	53	III	mutant	adeno	61.9
11148	F	63	II	wild-type	adeno	26.6
11157	M	73	II	wild-type	adeno	130.1
11275	M	76	II	wild-type	adeno	90.4
11692	M	58	III	mutant	adeno	112.3
11731	M	59	III	mutant	mucinous	18.4
11854	M	70	III	n.d.***	adeno	18.8
11873	M	72	II	wild-type	adeno	106.7
11918	M	59	II	wild-type	adeno	104.9
12004	M	51	III	mutant	adeno	102.1
12031	M	50	II	wild-type	adeno	38.9
12051	M	70	II	wild-type	adeno	79.1
12076	M	76	II	mutant	adeno	100.1
12124	M	60	III	mutant	adeno	98.6
12158	M	70	III	wild-type	mucinous	97.9
12163	M	53	III	mutant	adeno	5.9
12169	M	67	II	wild-type	adeno	97.2
12375	F	66	III	wild-type	mucinous	92.2
12879	M	80	I	mutant	adeno	62.8
12892	M	69	I	wild-type	adeno	79.9
13201	F	60	I	mutant	adeno	72.4
13547	M	69	I	wild-type	adeno	55.5
13799	M	44	II	wild-type	adeno	61.2
14278	M	59	I	mutant	mucinous	54.1
14554	M	59	I	mutant	adeno	50.1
15059	M	67	I	wild-type	adeno	43.5

* Schetter *et al*., JAMA 299: 425-436, 2008.

** p53 status was assumed to be 'wild-type' or 'mutant' by immunohistochemical staining of p53 and MDM2 (Costa *et al*., J. Pathol. 176: 45-53, 1995; Nenutil *et al*., J. Pathol. 207: 251-259, 2005).

*** Not determined.

Supplementary Table S4.

Δ133p53 and p53β expression in p53 'wild-type' and 'mutant' cases of colon carcinoma*.

Case-stage	Δ133p53		p53β	
	Non-ca	Carcinoma	Non-ca	Carcinoma
p53 'wild-type'				
10167 - I	0.0285	0.2276	0.0985	0.0372
12892 - I	0.1376	0.0892	0.0868	0.0208
13547 - I	0.4270	0.1329	0.0292	0.0546
15059 - I	0.0816	0.2083	0.1828	0.0647
10212 - II	0.0302	0.1529	0.0723	0.0512
11148 - II	0.1458	0.1007	0.0132	0.0639
11157 - II	0.3105	0.9175	0.0489	0.0480
11275 - II	0.0986	0.4103	0.0813	0.0560
11873 - II	0.3557	0.7519	0.0088	0.0338
11918 - II	0.0885	0.4647	0.2323	0.0661
12031 - II	0.4436	0.5961	0.0447	0.0530
12051 - II	0.2774	0.0122	0.1025	0.0169
12169 - II	0.1679	0.6279	0.0742	0.0271
13799 - II	0.0033	0.3206	0.0488	0.0633
12158 - III	0.2558	0.5446	0.1255	0.0317
12375 - III	0.0944	0.2126	0.0633	0.0667
p53 'mutant'				
12879 - I	0.2421	0.0033	0.0416	0.0021
13201 - I	0.1807	0.3560	0.0629	0.0513
14278 - I	0.3356	0.2461	0.0658	0.1244
14554 - I	0.1567	0.2301	0.1134	0.0460
12076 - II	0.3786	0.3812	0.2232	0.0418
10186 - III	0.4134	0.0396	0.1345	0.0060
10515 - III	0.1003	0.0033	0.0617	0.0118
11692 - III	0.6377	0.4520	0.0347	0.0220
11731 - III	0.1403	0.0737	0.0213	0.0248
12004 - III	0.2440	0.2460	0.0457	0.0281
12124 - III	0.3315	0.5139	0.0309	0.0034
12163 - III	0.2377	0.5289	0.0798	0.0370

***Normalized values of Δ133p53 and p53β expression (normalized with β-actin) were from quantitative analysis of the results shown in Supplementary Fig. S8a and S8b.**